



# Groundwater exploration in a typical southwestern basement terrain

C. C. Okpoli and P. Ozomoge

Department of Earth Sciences, Faculty of Science, Adekunle Ajasin University, Akungba-Akoko, Nigeria

## ABSTRACT

Integrated geophysical techniques were applied for groundwater exploration in a typical southwestern Nigeria basement terrain. EM-3D was primarily used to map out the precise subsurface conductive zones before adopting the recommended sounding locations with aid of Vertical Electrical Sounding (VES) technique. Hydraulic parameters were also estimated and plotted. Twenty Electromagnetic (EM) horizontal profiling and Schlumberger methods were conducted in E-W and N-S direction across the site. The points where the inflection of the raw real intersects the positive peak of the filtered real are diagnostic of major conductive zones suspected to be faults/fractures. Possible groundwater flow paths that identified as conductive zones were used in picking locations for VES deep sounding. The VES conducted on the conductive zones, which are labelled  $V_1$ ,  $V_2$ ,  $V_3$  and  $V_4$  were characterised by good aquifer resistivity values with relatively thick overburden, which are the major factors in determining the groundwater potential of an area in a typical basement complex, while those carried out on the non-conductive zones labelled  $V_5$  and  $V_6$  were characterised by poor indication to groundwater potential of the area.

## ARTICLE HISTORY

Received 3 September 2019  
Revised 18 February 2020  
Accepted 25 February 2020

## KEYWORDS

Electromagnetic; VES;  
hydraulic parameters;  
Schlumberger; groundwater

## 1. Introduction

Groundwater is a mysterious nature's hidden treasure. Its exploration and exploitation have continued to remain an important issue due to its unalloyed needs. Though there are other sources of water, like streams, rivers, ponds, etc., none is as hygienic as groundwater because groundwater has an excellent natural microbiological quality and generally adequate chemical quality for most uses (Okpoli 2017). To unravel the mystery of groundwater, a detailed geophysical and hydro-geological understanding of the aquifer types and their spatial distribution are paramount in order to characterise the hydraulic zones in an area. The university communities, for example, Adekunle Ajasin University, Akungba-Akoko are underlain by the Basement Complex rocks of the Southwestern Nigeria. It is bounded in the East and South by neighbouring town of Iwaro-Oka and Etioro-Supare Akoko respectively.

Akungba- community has witnessed an exponential increase in population of various groups of people in recent times due to the relocation of a state university to Akungba- Akoko few years ago; this caused astronomical demand of water, since available confined and unconfined water resources may not be adequate. Premium attention must be paid to the management and sustainability of productive deeper aquifers to meet the challenging needs. The study area being within a typical southwestern basement geologic setting requires a critical understanding of the hydrogeology and integration of geophysical data types to effectively characterise the

hydro-geologic zones and to enhance successful identification of deeper aquifers and wells (Omosuyi et al. 2003).

Several authors have noted that electromagnetic (EM) survey is best used in areas of crystalline Basement rocks for mapping areas of fractures and/or weathered materials of the Basement Complex which are often the significant water bearing layers directly overlying the fresh basement rocks. EM prospecting has been found useful as a conductive tool for mineral and groundwater exploration EM34-3D is fast, and requires less labour, and above all covers a large area in a short time. EM profiling and Vertical Electrical Sounding (VES) geophysics have been complementarily used in the delineation of basement regolith, fissured media, and associated deep weathered zones. Many authors have immensely employed electrical resistivity techniques for hydro-geologic investigations coupled with EM tool for a typical basement terrain such as; (Adelusi et al. 2009; Adiat et al. 2009; Erram et al. 2010; Alisiobi and Ako 2012; Okpoli and Odundun 2016; Okpoli and Tijani 2016).

This work applied integrated EM and electrical resistivity geophysical techniques in mapping out water bearing zones with distinct diagnostic structures in solving communal water scarcity.

## 2. Description of the study area

The study area is located within Akoko region, Ondo State of Nigeria, lies between latitudes  $07^{\circ} 25.89$ ,  $07^{\circ}$

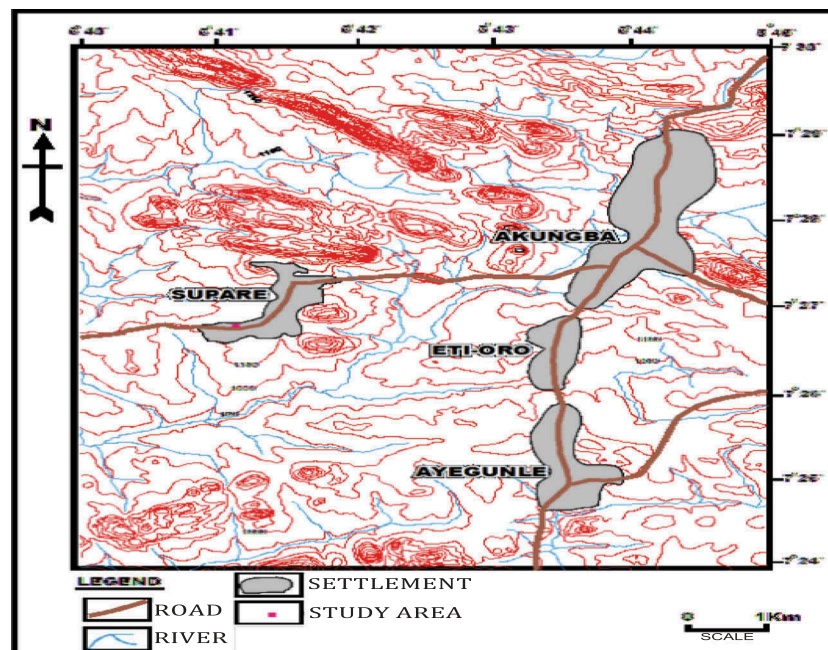


**Figure 1.** Topographic maps of Akungba-Akoko and its environs.

25.87° N and Longitude 05° 40.44, 05° 40.43°E (Figure 1). It covers an estimated area of about 30 square kilometres. It has an approximated elevation of about 340 m and enclose within the Nigeria topographic sheet 255 (Owo Sheet).

The accessibility of this area is good as a result of the presence of good road network. There is a major tarred road that dissect the area in the East to west direction which is a major road running from Akungba Akoko, Ondo State. There are other untarred but motorable roads, which also aid accessibility in the area. Some of the river courses dried up during dry season, thus making it easier to study rock exposures along river courses in the mapped area. Road cut and footpaths also make the rocks available for study.

The study area is characterised by the tropical Savannah climate. This climate exhibits well-marked rainy season and dry season. The rainy extends from late March to early October and the annual rainfall is about 1500 mm per annum while the dry season extends from December to March. The samples were collected during the wet season, which was around April. The study area, Akoko towns and its environs fall into the Guinea savannah vegetation belt.

The drainage pattern in the study area is dendritic. This major river has North-South flow direction and is often meandering and contains a lot of tributaries. The area has little systems, which take their source from the hills in the northern part while the streams river channels and erosion flow south-eastward. Most of these streams are meandering which reveals the nature of hard crystalline rock in the area thereby controlling the direction of flow. The topography of the area is characterised by high lands and low lands where, the

Northern part having topographically higher elevations than the Southern parts. The highlands are made up migmatite gneiss rocks, which form inselbergs while the lowlands are valleys and plains covered by laterite. The highest elevation in the region is slightly over 1820 ft above the sea level.

The study area lies within the crystalline Basement Complex rocks of Southwestern Nigeria (Figure 2). The groups of the Basement Complex rocks identified within the Adekunle Ajasin University, Akungba -Akoko areas include: Migmatite Gneiss Quartzite Suite.

The study area is overlain by migmatite gneiss, a review of the rock type present and recognised by Rahaman (1988) is presented below. The migmatite-Gneiss quartzite complex is a heterogeneous rock group comprising quartzo-feldspathic gneiss and migmatite with grade of basic and calcareous, schist, marbles and quartzite known as Ancient meta-sediments or older meta-sediments (Rahaman and Ocan 1978).

The main rocks recognised in the study area are: Grey gneiss, Granite gneiss, Migmatite, Charnockite, Diorite, Pegmatite. The study area has suffered from various phases of deformation that led to the development of structures like foliations, faults, folds, lineation and joint among others.

### 3. Materials and methods

The geophysical prospecting methods adopted for this research work are: EM and VES using the equipment of EM34 -D and ABEM SAS-1000 Terrameter, respectively (Figure 3). Through the electrical resistivity method, the Schlumberger array was applied along with four metal electrodes, hammer, and four reels of connecting cables, tape rules, cutlass, clips, GPS and

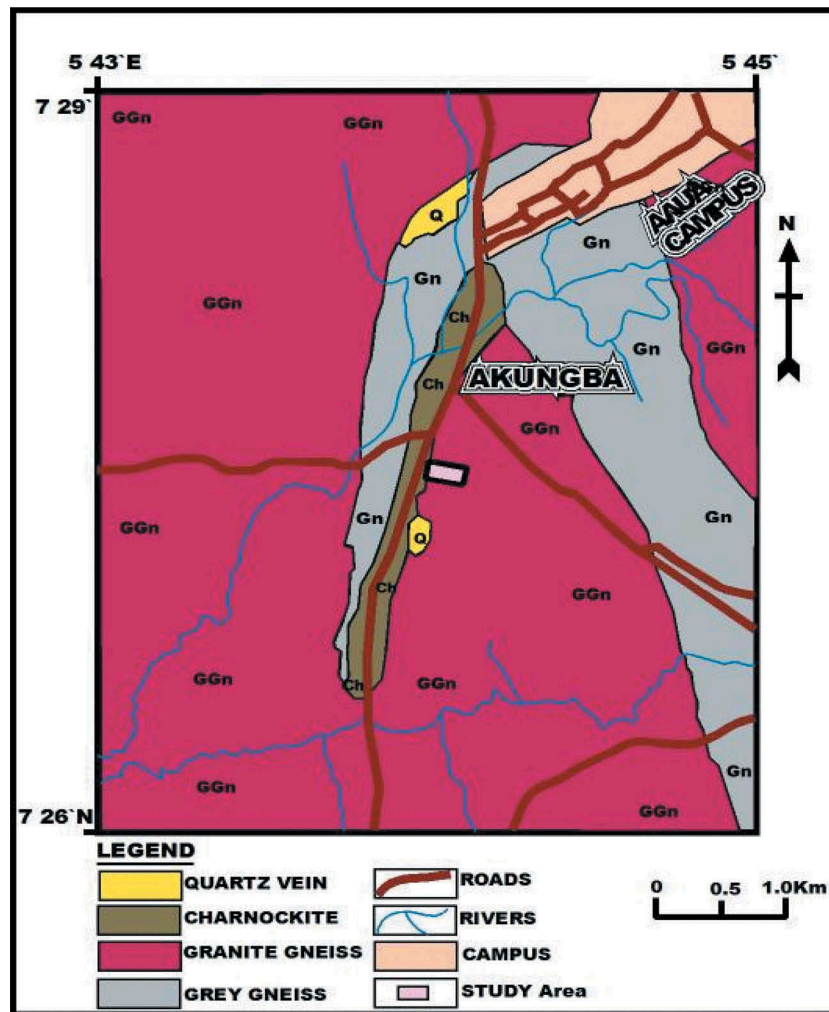


Figure 2. Geological map of Akungba-Akoko area.

rope. Global positioning system (GPS) coordinates were collected; which were used to produce the base map. Figure 4 shows the acquisition map of both EM profiles and VES stations in the study area. The GPS data were collected with a spacing interval of about 40 m, the data was processed using Surfer 12 software, and the base map was produced.

### EM 34-3D EM s Survey

The equipment used in EM survey include: The Transmitter: This device transmits EM wave into the earth to generate the secondary wave while the Receiver receives EM wave from the transmitter into the earth to generate the secondary wave and two coplanar coils for vertical and horizontal conductivity.

In any EM survey, a consideration of the depth of penetration of the EM radiation and the resolution as a function of depth is very paramount (Kearey et al. 2002; Milsom 2003). The depth of penetration is mostly a function of the conductivity and frequency of the media through, which EM radiation is transmitted. Depth of penetration, otherwise known as skin depth is defined as the depth at which the amplitude of a plane wave has decreased to  $1/e$  or 37% relative to its

initial amplitude  $A$  (Milsom 2003). Mathematically, the amplitude of EM radiation as a function of depth ( $z$ ) relative to its original amplitude  $A_0$  is:

$$A_z = A_0 e^{-1}$$

The mathematical expression of skin depth is given by:

$$\delta = \sqrt{\frac{2}{\omega\sigma\mu}} = 503\sqrt{(f\sigma)}$$

where  $\omega = 2\pi f$ ,  $f$  = frequency in Hz,  $\sigma$  = conductivity in S/m and  $\mu$  = magnetic permeability (usually  $\approx 1$ ) A realistic estimate of the depth to which a conductor would give rise to a detectable EM anomaly is  $\approx \delta/5$  (Reynolds 1997). EM34-3D used 6.4 KHz frequency with 10 m spacing and its skin depths of their FEM systems as a function of the inter-coil separation.

### 3.1. VES survey

Measurements of apparent resistivity are made by systematically varying electrode spacing. This procedure is called VES, where a fixed point is being probed with respect to depth. The midpoint of the array is





**Figure 3.** Taking measurement with GEONICS EM 34-3 and Terrameter ABEM SAS 1000.

kept fixed while the distance between the current electrodes is progressively increased. This causes current lines to ever penetrate greater depths, depending on the vertical distribution of conductivity (Lowrie 2007). A maximum electrode spread ( $AB/2$ ) of 65 m was used, and a total of 20 VES was carried out in the study area. Each VES soundings were recorded in a Schlumberger electrical resistivity data sheet.

The Schlumberger depth sounding data acquired are presented as curves, geo-electrical sections. This is achieved by plotting the apparent resistivity values against the electrode spacing on a bi-log graph and plotting the resistivity values with respect to depth for each VES station. The qualitative interpretation involves the inspection of geo-electrical sections, maps and sounding curves, for signatures or pattern diagnostics of a particular target. The quantitative

interpretations of field curves were initially carried out using the convectional partial curve marching techniques using auxiliary point methods. This process provides the estimates of resistivity and thickness of various geo-electrical layers. These parameters are used as starting models for the computer iteration.

The process involves matching the sounding curves segment by segment with theoretical curves of Orellana and Mooney 1972. The technique is an empirical method by which a multi-layered case is progressively reduced to a simple two or three-layer case. Each sounding curve is super-imposed on the master curve and with the axis kept parallel; it is moved about until a fit is obtained over as many as possible. The point of intersection of the master curve is marked on the field curve tracing paper where the resistivity and the thickness of the first layer are

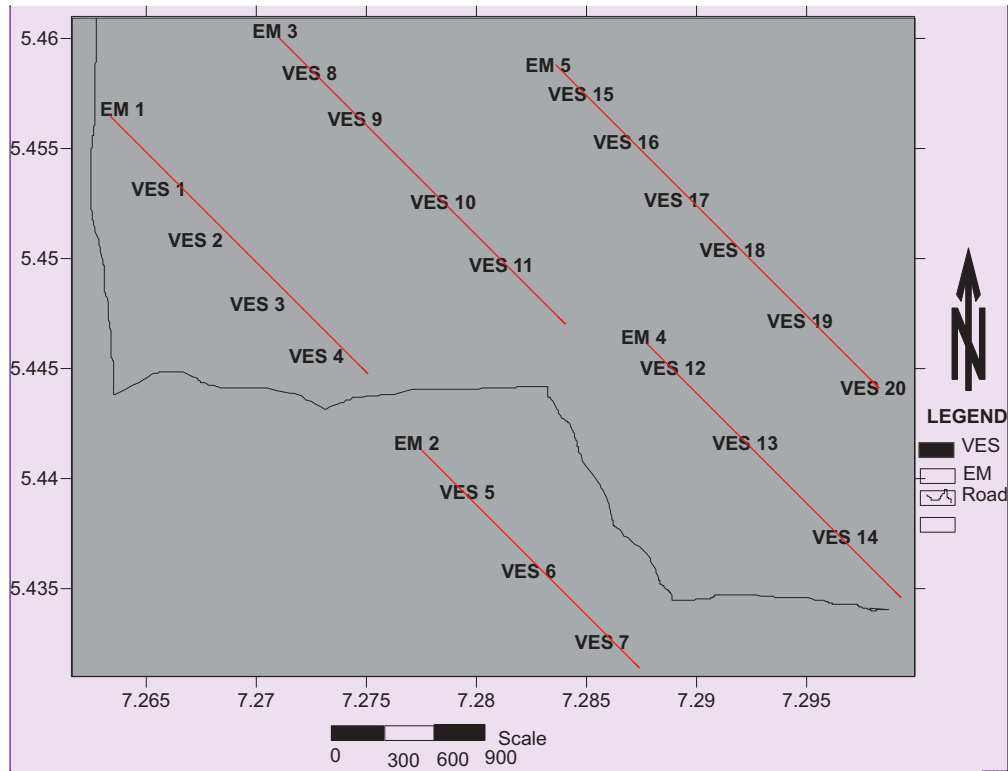


**Figure 4.** Acquisition map of EM profiles and VES stations for groundwater prospecting.

obtained. The value of  $K$  (which is the reflection coefficient at the interface between the first and second layer) on the master curve that fitted the first segment is noted. The values of the layer thickness and resistivity obtained through curve matching serve as starting models which are input into computer using Win Resist version 1.0 (1988–2004). The results of the 20 VES interpretations and EM survey data obtained after iteration. The model parameters were modified where necessary until satisfactory fit was obtained in each case.

The general expression for calculating layer resistivity ( $\rho_n$ ) and thickness ( $h_n$ ) (Omosuyi and Enikanselu 1991) is given as:

$$\rho_n = \rho_{(n-1)r} \times K_{n-1}$$

$$\rho_n = \rho_{(n-1)r} \times \frac{D_n}{D_{r(n-1)}}$$

for  $n = 2$ , or  $n = 3$

$$\rho_2 = \rho_{2-1} \times K_{2-1}$$

$$\rho_2 = \rho_1 \times K_1$$

$$\rho_3 = \rho_{3-1} \times K_{3-1}$$

$$\rho_3 = \rho_{2r} \times K_2$$

Similarly,

$$h_2 = h_1$$

$$h_2 = h_1 \times \frac{D_r}{D_{r2}}$$

$$h_3 = h_{2r} \times \frac{D_n}{D_{r2}}$$

Where,

$\rho_n$  = apparent resistivity of the  $n$ th layer

$h_n$  = thickness of the  $n$ th layer

$\frac{D_n}{D_{r(n-1)}}$  = Depth ratio

$K_1$  = Reflection coefficient

$\rho_1$  = Apparent resistivity of the first layer

$\rho_2$  = Apparent resistivity of the first second layer

$\rho_{2r}$  = Replacement resistivity of the second layer

$\rho_{(n-1)r}$  = Replacement resistivity of the  $n$ th layer

$h_1$  = Thickness of the first layer

$h_2$  = Thickness of the second layer

$h_{2r}$  = Reflected thickness of the second layer

The various curve types show the qualitative interpretation of the VES data, four curve types were identified within the study area: A, H, Q, and QH-type curves.

## 4. Results and discussion

### 4.1. Discussion of EM results

#### 4.1.1. Interpretation of EM profiles and 2-D models

Profiles of raw real components and Q-factor values in percentages were plotted against station positions at regular intervals as shown in Figures 5–11. The values of the raw real were obtained directly from the EM34-3D equipment. The values of the Q-factor filtered operator were obtained through an established rule  $\{Q = (Q_4 + Q_3) - (Q_2 + Q_1)\}$ .

In the profiles, the positive peak of the Q-factor values were interpreted as conductive zones, which might be as result of geologic features such as fractures, faults, geologic contacts or weathered basement (Fraser 1969; Kaikkonen and Sharma 1997).

The varying amplitude (peak positive) which is a measure of the anomaly changes in the subsurface vary considerable across the study area, indicating variable conductivity changes of the subsurface materials.

From the EM Anomaly profiles, it can be deduced that positive peak anomalies are signatures of conductive zones while the negative peak anomalies are signatures of resistive zones across the study area. To clarify these positive peaks of the conductive anomalies, a number of VES stations were carried out at the sites of these peaks.

However, the corresponding 2-D models of the EM profiles along five traverses covering the study area were generated using a computer package called the KHF FILT (Karous-Hjelt and Fraser Filter programme) (Karous and Hjelt 1983). The conductive targets are shown as colour codes increases from left to right (i.e. from negative to positive). Features of varying degree of conductivity trending in different directions were delineated on the 2-D sections.

The results obtained from the processing/interpretation of the data are presented as geo-electrical

section and EM from which the relevance of these results used in evaluating the thickness, lateral extent and the EM properties within the campus (AAUA).

The results obtained from the interpretation of the EM and VES data acquired from the study area were used to draw geo-electrical sections (Figures 5–7). The profile trend N – S with length of approximately 200 m. The geo-electrical section draw along these profiles delineates three subsurface geologic layers. These include the top soil, the weathered layer and the fresh basement. The sections along the three profiles are marked by varying resistivity values.

#### 4.1.2. Qualitative and quantitative interpretation of EM profiles and sections

Figure 5(a,b) show EM profile and a 2-D inversion model along Traverse 1. The points where the inflection of the raw real intersect the positive peak of the filtered real were recorded on the EM profile at distance of 25, 45, 147 and 190 m, respectively, these points are favourable to the accumulation of groundwater in a typical basement complex. These positive peaks are indicative of the presence of fractured or conductive zone. The pseudo-section demonstrates the measure of the conductivity of the subsurface as a function of depth. The conductivity is shown as colour codes, with conductivity increasing from left to right (i.e. from negative to positive). Different characters of varying degrees of conductivity trending in different directions were delineated. Moderately thick conductive bodies were recorded in the 2-D inversion model.

Figure 6(a,b) shows EM profile and a 2-D inversion model along Traverse 2. The points where the inflection of the raw real intersect the positive peak of the filtered real were observed on the EM profile at distance of 25, 45 and 185 m respectively, these points are favourable to the accumulation of groundwater in a typical basement complex. These positive peaks are

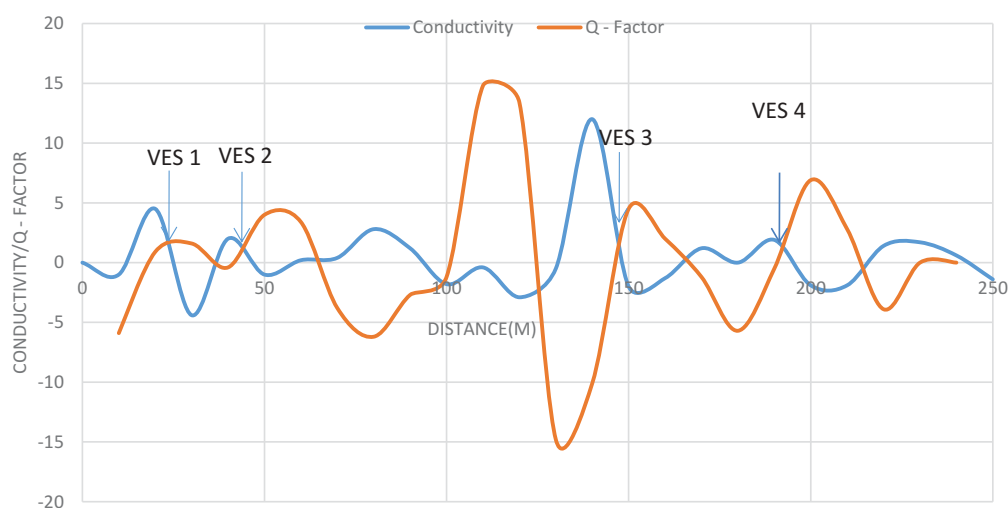
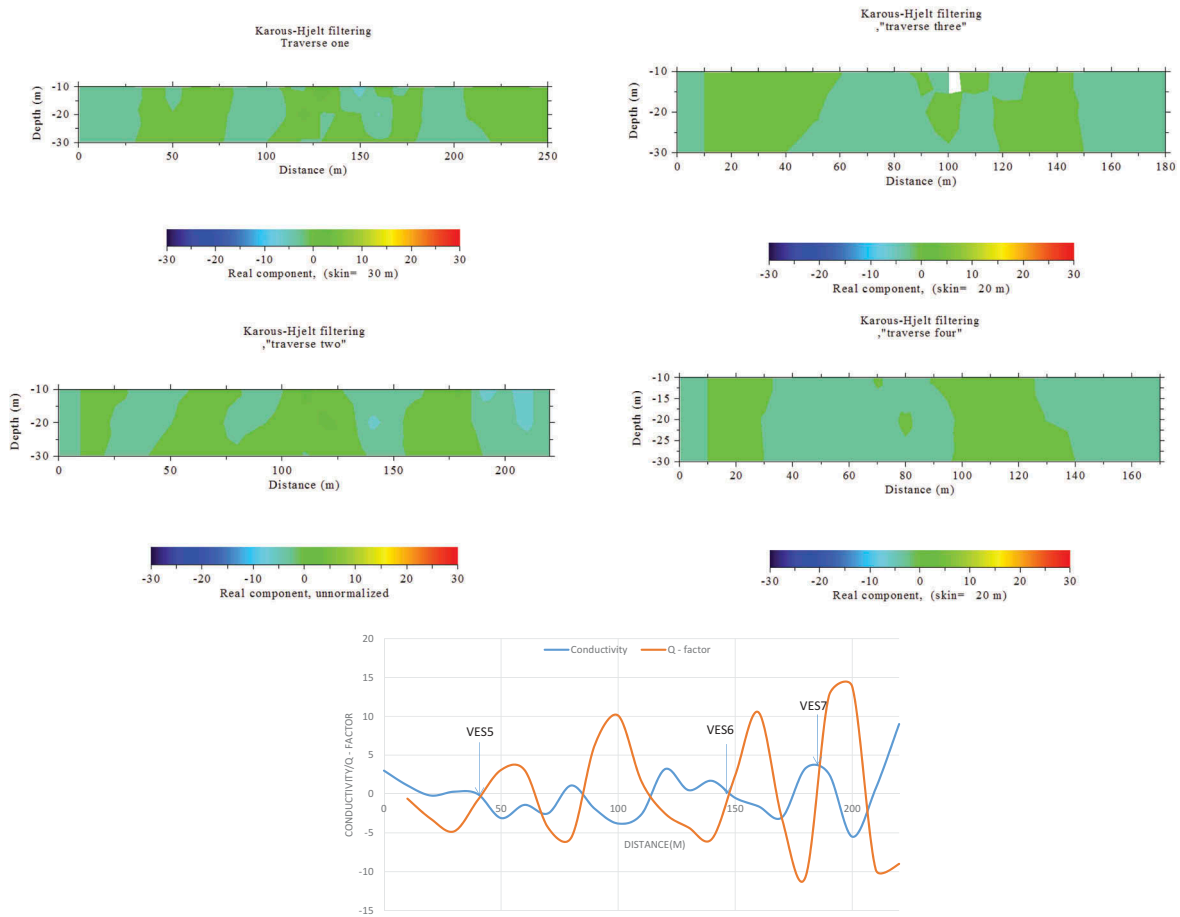


Figure 5. (a) EM profile (b) EM section along Traverse 1–4 (S–N).



**Figure 6.** (a) EM profile (b) EM section along Traverse 5–7 (S-N).

indicative of the presence of Fractured or conductive zone (McNeill and Labson 1991). The 2-D inversion model established the deduction from the EM profile about the presence of a relatively linear conductive structure at the established distances.

Figure 5, shows EM profile and a 2-D inversion model along Traverse 1 to 4. The points where the inflection of the raw real intersect the positive peak of the filtered real were observed on the EM profile, these points are favourable to the accumulation of groundwater in a typical basement complex. These positive peaks are indicative of the presence of fractured or conductive zone. The 2-D inversion model established the deduction from the EM profile about the presence of a relatively linear conductive structure at the established distance. Some highly resistive bodies were also observed on the section at distance 100, 205 and 440 m respectively, this could be a dyke structure, a contact zone or an intrusion.

Figure 7, shows EM profile and a 2-D inversion model along Traverse 8 to 11. The points where the inflection of the raw real intersect the positive peak of the filtered real were observed on the EM profile at distance of 40, 75, 118 and 150 m, respectively, these points are favourable to the accumulation of groundwater in a typical basement complex. These positive peaks are indicative of the presence of Fractured or

conductive zone. The 2-D inversion model established the deduction from the EM profile about the presence of a relatively thick linear conductive structure at the established distance. Some fairly resistive bodies were also observed on the section at various distances, this could be a dyke structure, a contact zone or an intrusion.

The EM profiles and sections were interpreted qualitatively and quantitatively as follows:

Figure 8 shows EM profile and a 2-D inversion model along Traverse 12 to 14. The points where the inflection of the raw real intersect the positive peak of the filtered real were observed on the EM profile at distance of 55, 77 and 132 m, respectively, these points are favourable to the accumulation of groundwater in a typical basement complex. These positive peaks suggest the presence of fractured or conductive zone. The 2-D inversion model recorded thick conductive linear structures (deep green) ranging from 20 to 30 m distances and some pockets of conductive bodies. More so, they are presence of fairly resistive bodies observed in the pseudo-section.

Figure 9, shows EM profile and a 2-D inversion model along Traverse 15 to 20. The points where the inflection of the raw real intersect the positive peak of the filtered real were observed on the EM profile at distance of 17, 40, 60, 110, 149 and 210 m, respectively,



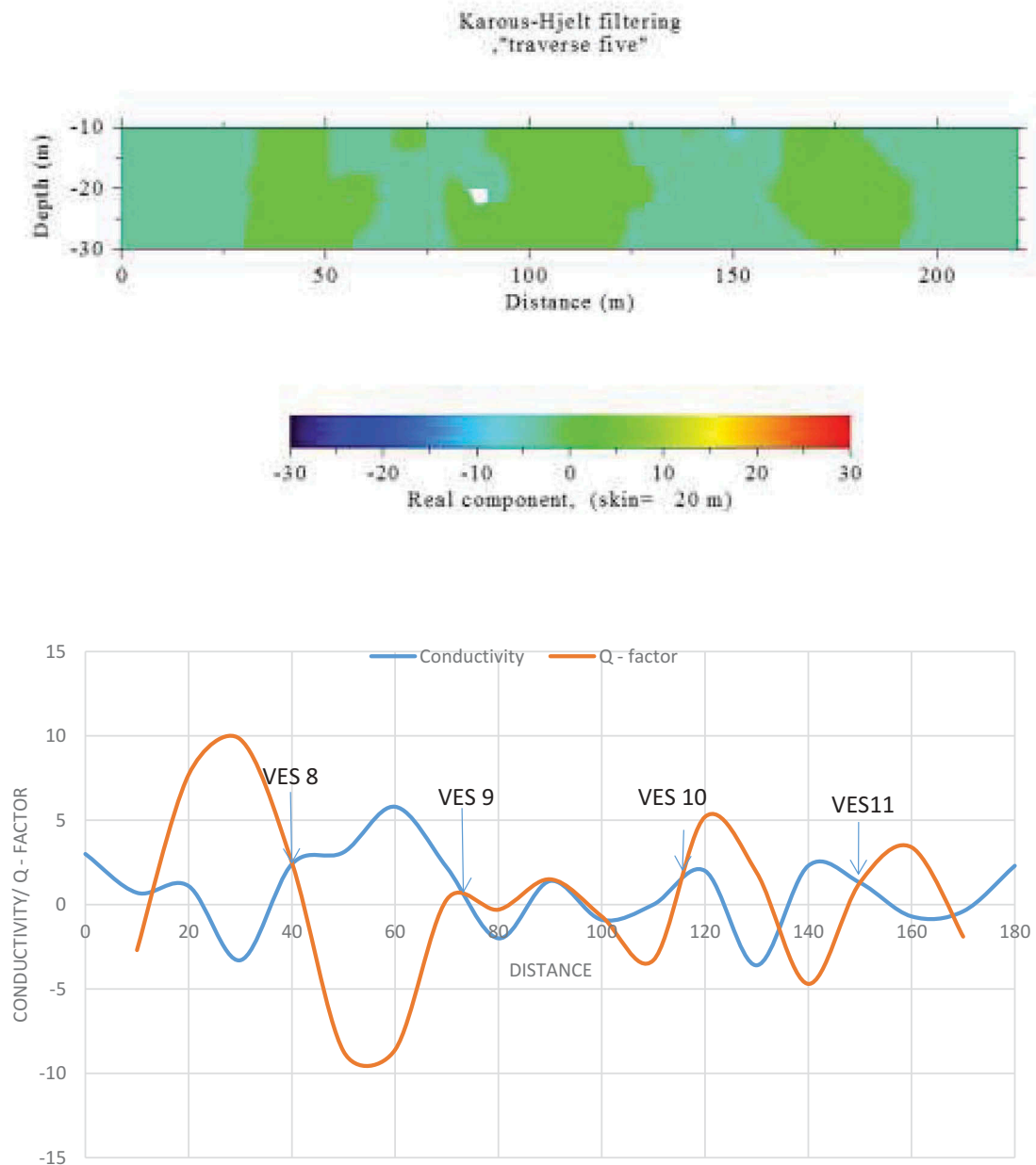


Figure 7. (a) EM profile (b) EM section along Traverse 8–11 (S-N).

these points are favourable to the accumulation of groundwater in a typical basement complex. These positive peaks are indicative of the presence of fractured or conductive zone. The 2-D inversion model recorded thick conductive linear structures (deep green) ranging from 20 to 30 m distances and some pockets of conductive bodies. More so, they are presence of fairly resistive bodies observed in the pseudo-section.

The high conductive zones in the study area is suggestive of fractured and interconnected joints witnessed during the EM surveys while the low conductive zone are probably due to fresh basement and non-conductive layers/lithologies. Interconnected fractures and joints are conductive because it favours groundwater accumulation while fresh basement and non-conductive intrusive bodies are resistive and do not favour groundwater accumulation. Preliminary EM

surveys are crucial in siting conductive zones. VES follow EM surveys in order to locate productive wells.

#### 4.2. Discussion of VES results

A total of 20 VES stations were carried out and the results are presented as: sounding curves, tables and geo-electric sections. However, the VES data were acquired using 25 m interval along each of the traverse.

##### 4.2.1. Sounding curves

The 20 sounding curves were classified into seven curve types: H, HA, KH, HK, HKH, HAK and QH curves, occurring in the proportion of 10:10:6:5:2:1:1, respectively.



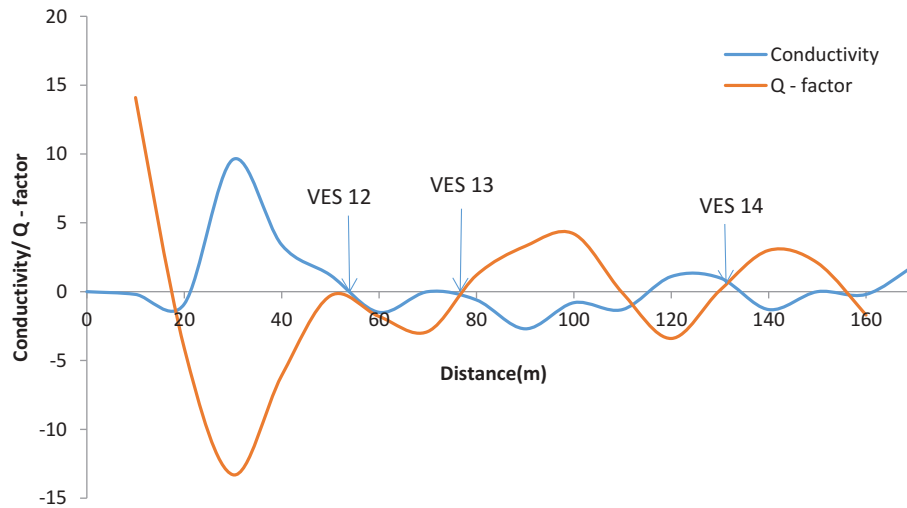


**Figure 8.** (a) EM profile (b) EM section along Traverse 12–14 (S-N).

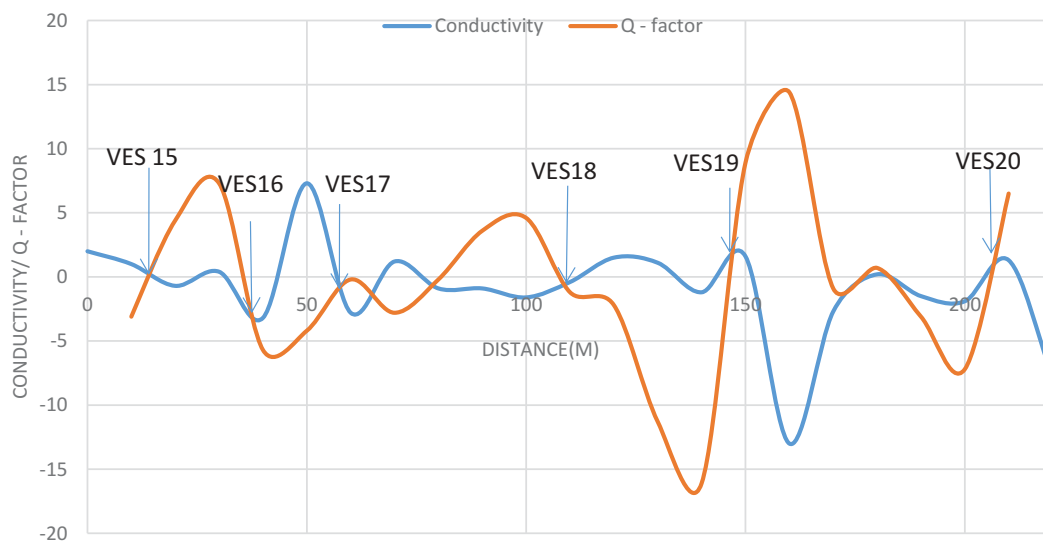


**Figure 9.** (a) EM profile (b) EM section along Traverse 15–20 (S-N).

Typical curve types are shown in Figures 10–12, geo-electric sections and parameters are demonstrated pictorially. The VES data interpretation delineates four major geologic units. These are the topsoil, the weathered layer, the fractured basement and the fresh basement as shown in the characteristic VES curves in figures. The sounding curves were characterised according to their signatures, which mirror the layering of the subsurface.

For VES 3 (Figure 10(c)), the top soil has a resistivity of 95  $\Omega\cdot\text{m}$  and a thickness of 0.5 m, below this is a lateritic clay layer having a resistivity of 171  $\Omega\cdot\text{m}$  with 1.4 m thickness, beneath this is a partially weathered layer with a resistivity of 105  $\Omega\cdot\text{m}$  with a thickness of 9.1 m. The aquifer unit for VES 3 is this weathered layer. Beyond this layer is the layer referred to as the fractured basement, with resistivity of 593  $\Omega\cdot\text{m}$  and with thickness at infinity. Considering the aquifer unit resistivity value with the overburden

thickness, VES 3 indicates a good groundwater potential in a typical basement complex.

#### 4.2.2. Geo-electric sections

The results obtained from the quantitative interpretation of the sounding curves were used to generate the geo-electric sections that are illustrated in Figures 13–17. The geo-electric sections show the distribution of the resistivity of the various mapped layers with respect to their distribution.

### 4.3. Constructed maps

#### 4.3.1. Conductivity maps

Figure 18(a,b) are the conductivity maps of the study area respectively; Figure 18(a) was generated by using the raw real data with the coordinates while Figure 18(b) made use of the filtered real data with the coordinates.

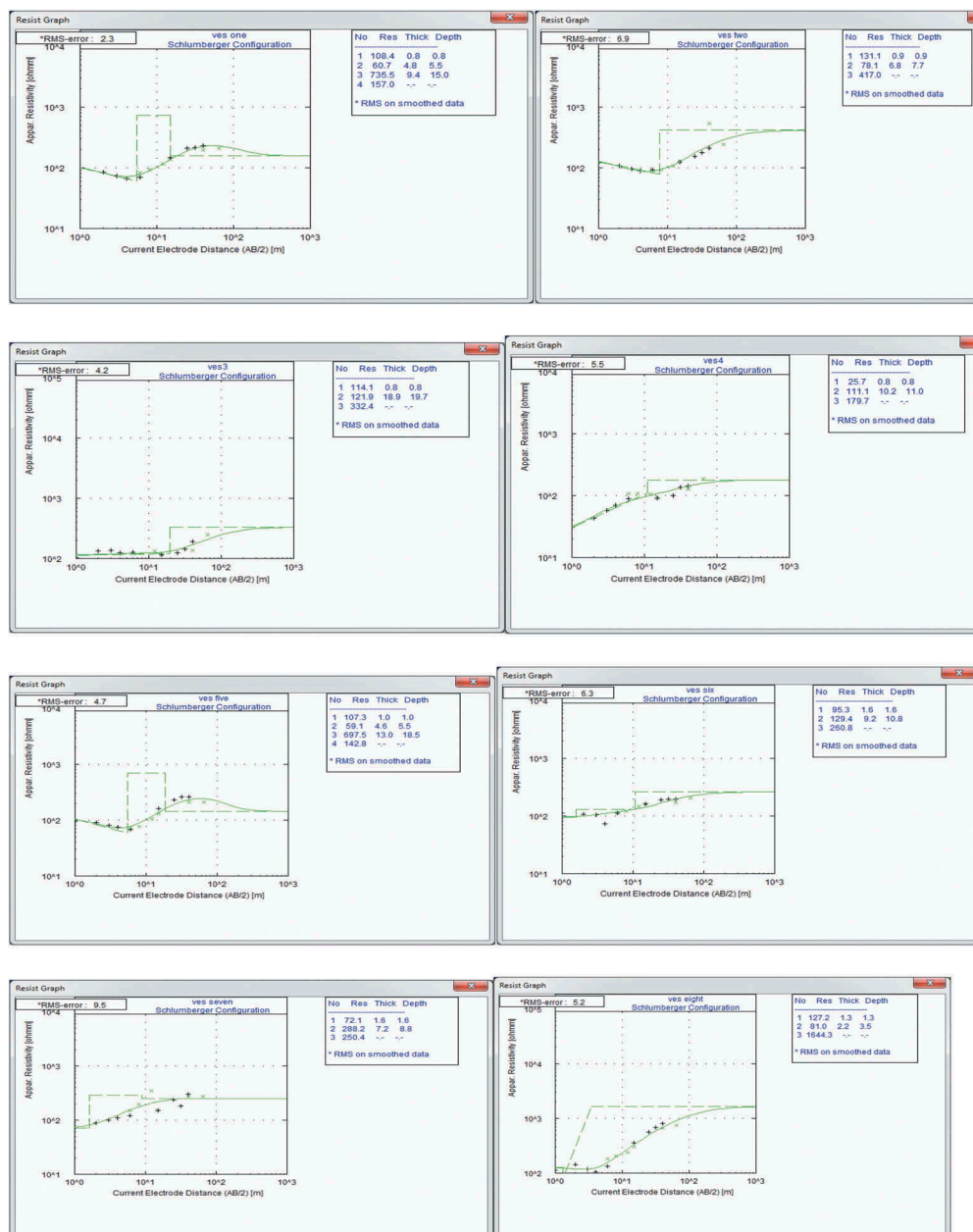


Figure 10. Typical VES curves over conductive zones- $V_1$ -  $V_8$ .

The contour lines were fairly distributed along the traverses within the study area, the interpretation is based on the colour codes as represented on the scale. The zones range from fairly conductive to highly conductive zones. Five major conductive zones were delineated occurring at north eastern, northern, north western and southwestern parts of the area respectively. Thus, the conductive zones established are relevant in groundwater development of the area.

#### 4.3.2. Structural map

The structural map shows the attitude of the fractures, four structural trends were highlighted on the study area as shown in Figure 19, and they are labelled  $FR_1$ ,  $FR_2$ ,  $FR_3$  and  $FR_4$ , respectively.

The  $FR_1$ , which cut through  $F_3$ ,  $F_4$ ,  $F_5$ , and  $F_6$ , trend approximately north western part of the study area is

found on the porphyritic granite. The  $FR_2$ , which cut across  $F_7$ ,  $F_8$ , and  $F_9$ , trend approximately north western/south western axis of the study area is also lying on the porphyritic granite. The  $FR_3$  correlates  $F_{18}$ ,  $F_{13}$  and  $F_{15}$ , and trend approximately northern/south eastern part of the study area, the northern part is found on the granite while the southeastern is lying on the migmatite gneiss rock and this indicate lithological boundary on the  $FR_3$  fracture trend. The  $FR_4$  correlates  $F_{10}$ ,  $F_{12}$ ,  $F_{14}$  and trend approximately southwestern/south-eastern part of the study area and also highlight geologic boundary between granite and migmatite gneiss rock.

The essence of the structural trend is to establish that the fracture zones in the study area are not localised but have a common distribution that aids correlation. Therefore, this map is relevant in groundwater and engineering geophysics such that where the

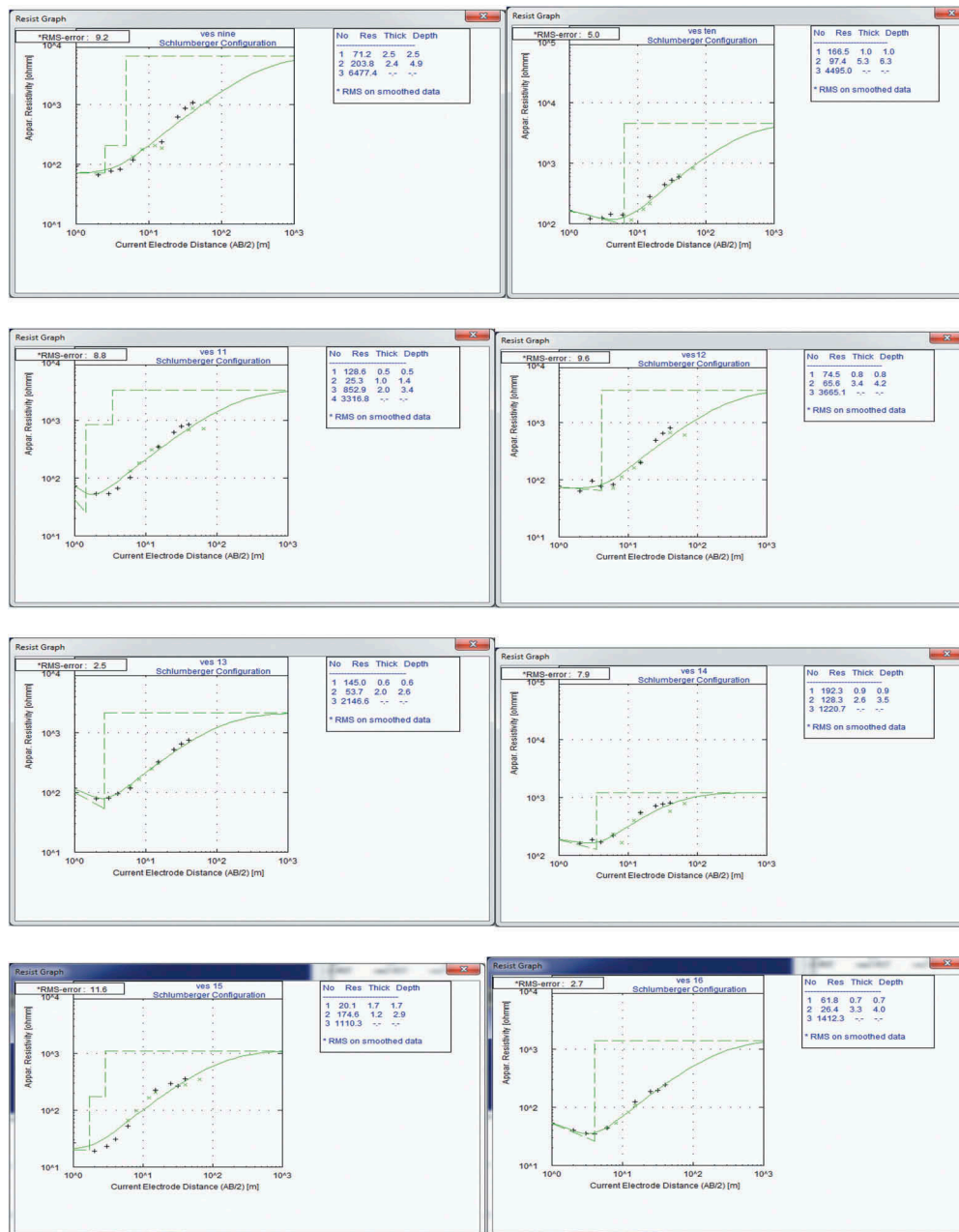


Figure 11. Typical VES curves over conductive zones-V<sub>9</sub>- V<sub>16</sub>.

presence of cross cutting fractures is observed, it is a good indicator and potential good site for groundwater abstraction.

#### 4.4. Validation of EM Results using VES

The results of the VES data coupled with the interpretation of the geo-electric parameters, four lithologic units, the top soil, clay/lateritic clay layer, weathered or fractured basement and fresh basement were delineated. The sounding curves obtained on the four conductive zones are HA, HKA, and KA curves, all with a good indication to groundwater prospect while that of the non-conductive zones are typical A curves which is characterised with relatively poor indication to groundwater potential.

It could be deduced from the VES analyses that the soundings that were carried out on the conductive zones i.e. V1,V2, V3 and V4 as prescribed by the EM method were characterised by a very good aquifer resistivity values and appreciable overburden thicknesses, which are the major factors in the determination of a typically good groundwater potential in a basement complex while on the other hand, the reverse was the case for the soundings conducted on the non-conductive zones i.e. V5 and V6.

Having considered the deduction from both the EM and VES results as analysed above, it could be inferred that the efficiency of the EM method as a reconnaissance tool in groundwater evaluation study is justifiable.

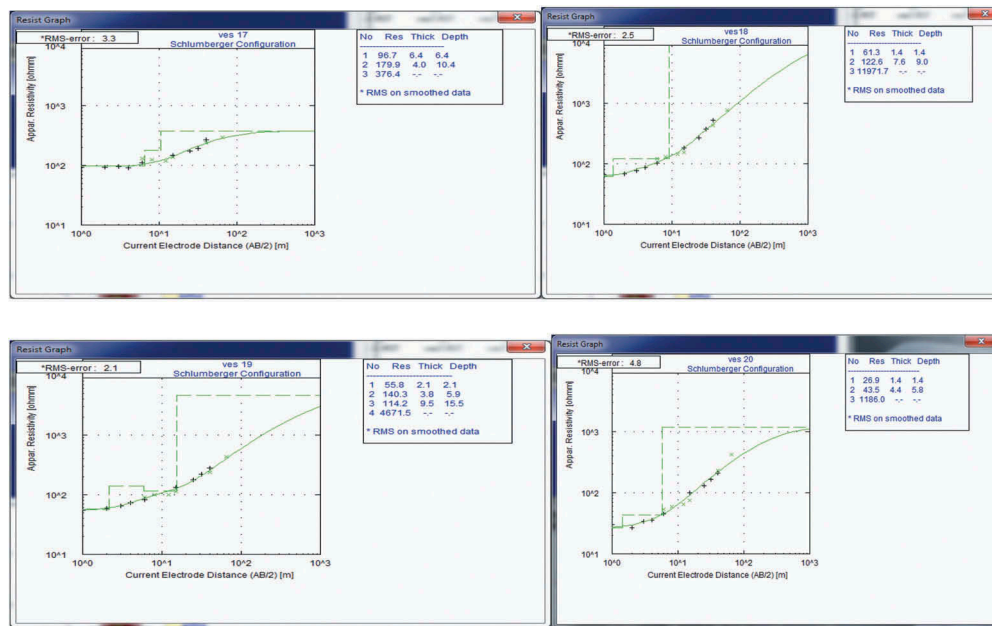


Figure 12. Typical VES curves over conductive zones-V<sub>17</sub>- V<sub>20</sub>.

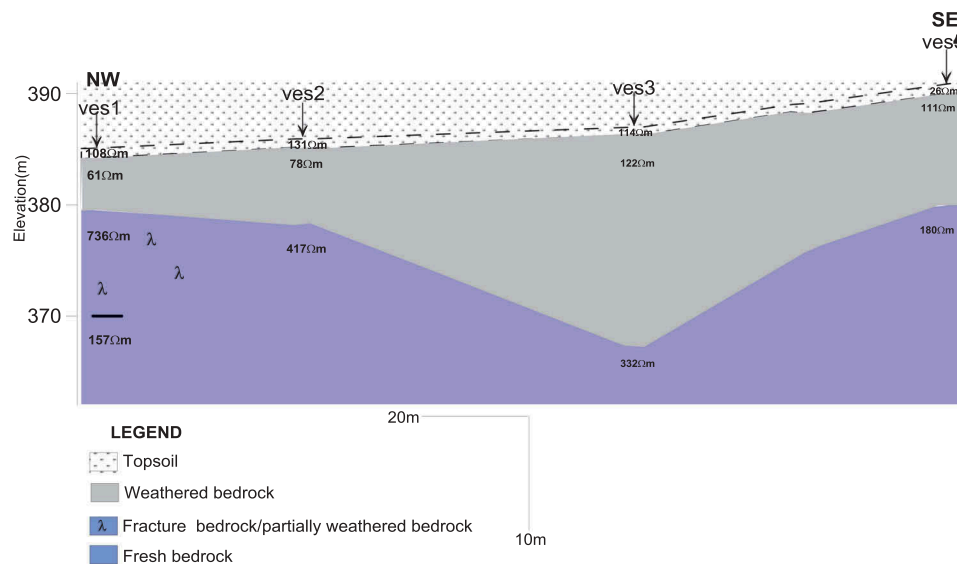


Figure 13. Geo-electric sections for VES 1-4.

#### 4.5. Estimation of hydraulic parameters from resistivity parameters

##### 4.5.1. Hydraulic conductivity

This refers to the ratio of the discharge velocity and corresponding hydraulic gradient. Mathematically, hydraulic conductivity can be expressed for porous zones as  $K (10^{-5}) = 95.5 - 1 \times \rho^{1.195} (M/S)$

Where  $K$  = hydraulic conductivity (m/s)

$\rho$  = resistivity of the porous media in ohm.m

Utilising the above relation, hydraulic conductivity was obtained for the whole 20 VES stations and the results are shown in Table 1. Figure 20 demonstrates the hydraulic conductivity that varied from aquifer to aquifer and range generally from  $0.31 \times 10^{-5}$  to  $9.89 \times 10^{-5}$  m/s. These low values

of hydraulic conductivity could be attributed to the clay content in the aquifer and the fact that the degree of hydraulic conductivity between the fractures are below.

##### 4.5.2. Transmissivity

This is the rate at which water flow through a vertical layer of the aquifer of unit width and extending full-saturated thickness under hydraulic gradient of 1.00

Mathematically, transmissivity ( $T$ ) can be expresses as

$$T = kh \text{ in } M^2/s$$

Where  $T$  = transmissivity

$K$  = coefficient of conductivity (m/s)



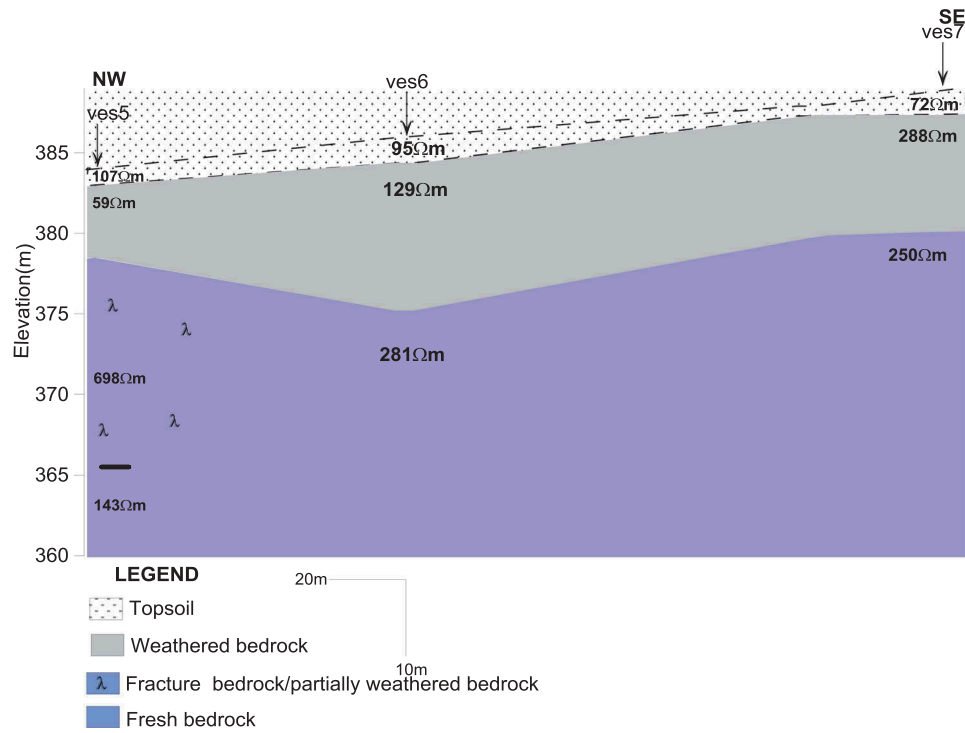


Figure 14. Geo-electric sections for VES 5–7.

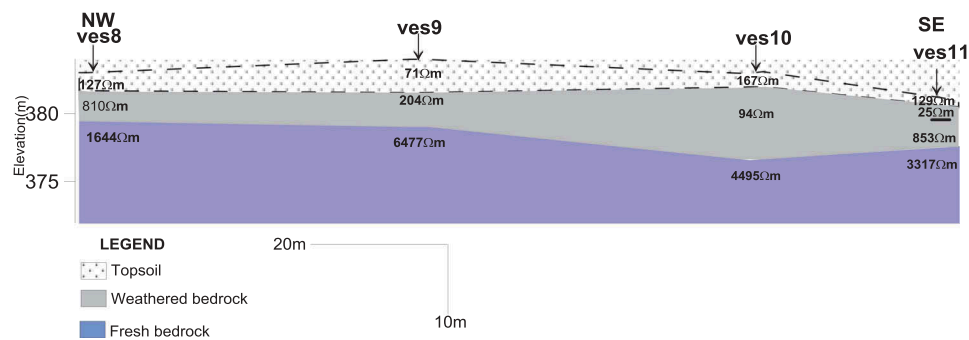


Figure 15. Geo-electric sections for VES 8–11.

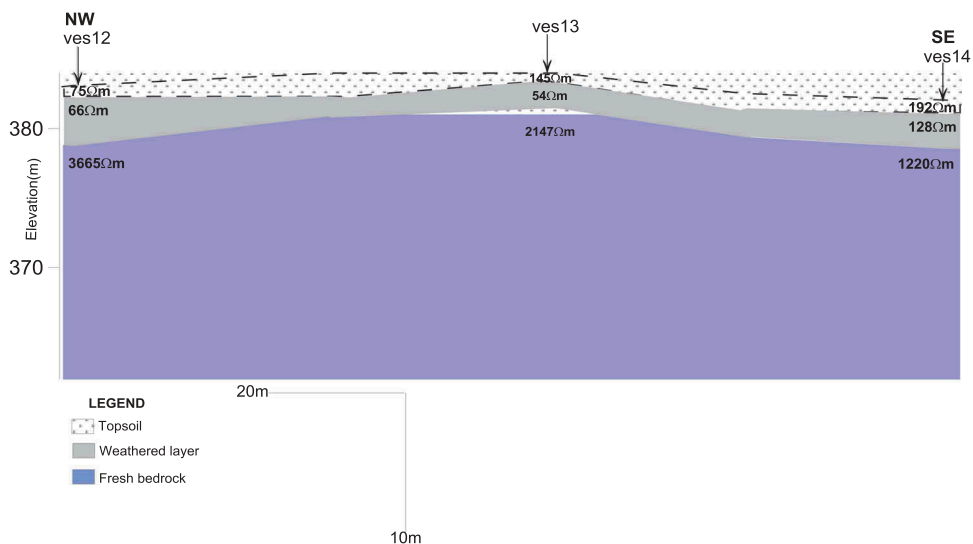


Figure 16. Geoelectric sections for VES 12–14.

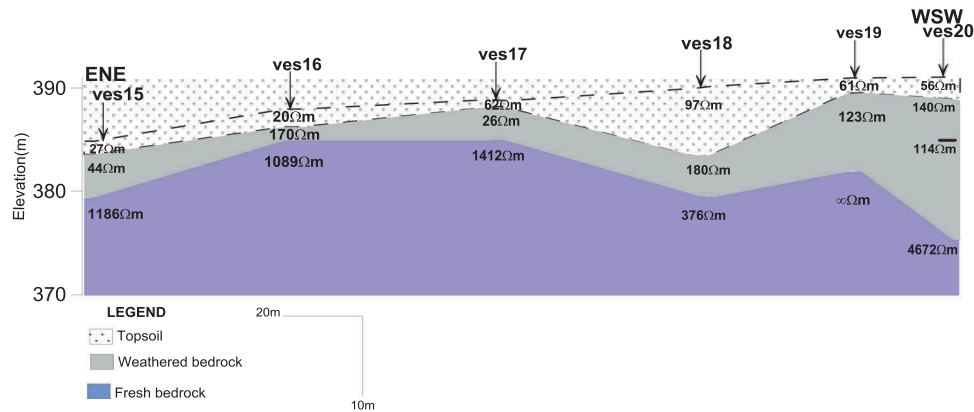


Figure 17. Geo-electric sections for VES 15–20.

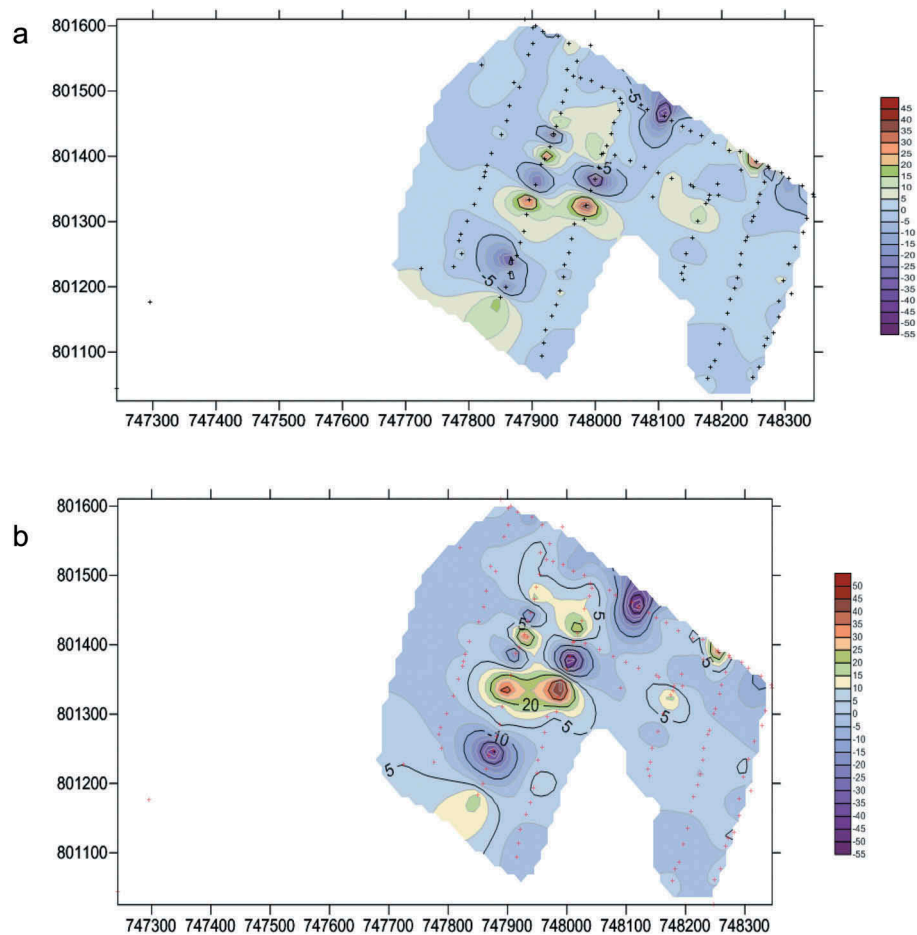


Figure 18. (a) Conductivity map of the area. (b) Conductivity map of the study area.

$H$  = aquifer thickness (m)

Estimates of transmissivity obtained from this approach in the study area shown that transmissivity ( $T$ ) range from  $0.78 \times 10^{-5}$  to  $450.3 \times 10^{-5}$  m/s. Table 1 and Figure 21 illustrate the transmissivity results of the VES stations

The values of both hydraulic conductivity and transmissivity are in good order because it was calculated for the whole saturated thickness of the aquifer. The fracture/weathered nature of the basement rock have direct implications for the relatively high transmissivity values.

#### 4.6. Isopach map of the overburden

The overburden as used in the text comprises of all materials above the presumably fresh bedrock. The map (Figure 22) showed the overburden thickness between 4.1 and 55.2 m.

The overburden is relatively thickness around the southwestern part of the study area (25.1–56.4 m). Generally, the overburden is relatively shallow when compared to the range given by (Olorunfemi and Okhue 1992; Dan-Hassan and Olorunfemi 1999 and Omosuyi et al. 2003), overburden thickness <30 m as

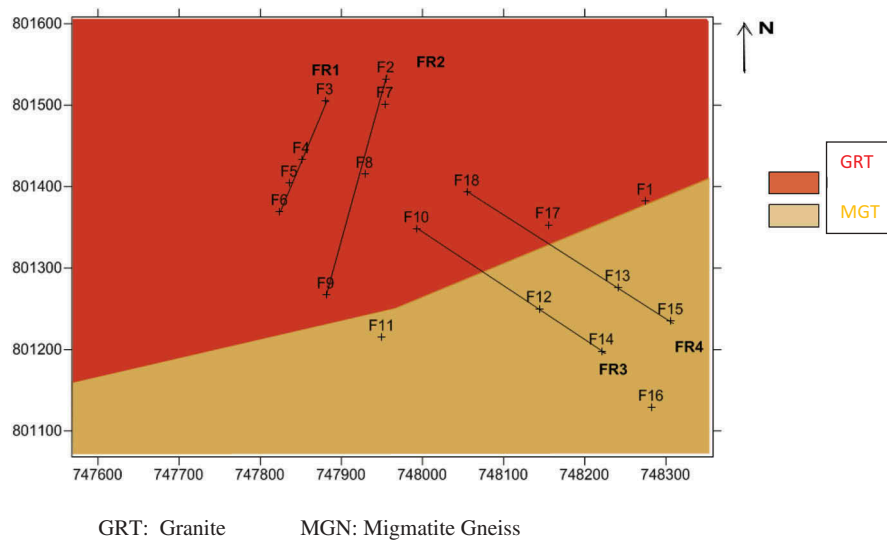


Figure 19. Structural map of the area.

Table 1. Hydraulic parameters.

| S/N | Latitude | longitude | Hydraulic conductivity<br>x 0.00001 m/s | Transmissivity<br>x0.00001 m/s | Bedrock<br>Relief (m) | Resistivity of<br>Bedrock (Om) | Total<br>traverse | Elevation | Overburden<br>Thickness | Longitudinal<br>unit |
|-----|----------|-----------|---|--------------------------------|-----------------------|--------------------------------|-------------------|-----------|-------------------------|----------------------|
| L1  | 072616   | 054310    | 8.10                                    | 7.51                           | 242.1                 | 509                            | 233               | 285       | 0.8                     | 216                  |
| L2  | 072644   | 054435    | 2.02                                    | 50.2                           | 234.5                 | 402                            | 241               | 283       | 6.8                     | 248                  |
| L3  | 072765   | 054499    | 2.97                                    | 63.23                          | 180.1                 | 533                            | 251               | 287       | 18.9                    | 218                  |
| L4  | 072837   | 054477    | 5.84                                    | 37.4                           | 190.6                 | 621                            | 261               | 277       | 10.2                    | 211                  |
| L5  | 072977   | 054488    | 3.38                                    | 51.5                           | 176.1                 | 841                            | 230               | 276       | 4.6                     | 198                  |
| L6  | 072979   | 054577    | 4.22                                    | 59.6                           | 198.3                 | 859                            | 252               | 283       | 8.9                     | 189                  |
| L7  | 072985   | 054588    | 5.46                                    | 45.9                           | 203.1                 | 735                            | 248               | 291       | 11.3                    | 222                  |
| L8  | 072993   | 054592    | 6.24                                    | 50.1                           | 231.5                 | 649                            | 233               | 289       | 20.4                    | 263                  |
| L9  | 072999   | 054598    | 7.28                                    | 66.7                           | 222.6                 | 559                            | 244               | 280       | 21.1                    | 188                  |
| L10 | 07283    | 054610    | 3.78                                    | 33.9                           | 252.7                 | 832                            | 263               | 279       | 15.3                    | 195                  |

thin overburden and overburden >30 m as thick overburden.

Related hydrogeophysical studies in similar geologic terrain (Olorunfemi et al. 1991; Dan-Hassan and Olorunfemi 1999 and Omosuyi et al. 2003) have identified areas with thick overburden cover as high groundwater potential zones. Hence, groundwater subtraction from the weathered basement aquifer is feasible in this area because the overburden thickness serves as recharge zone for the fractured aquifer.

#### 4.7. Longitudinal unit conductance (S)

A contour map of longitudinal conductance (S) values was prepared by using the relativity data as shown in Figure 23. It clearly demarcates region with longitudinal unit conductance and region with low longitudinal unit conductance. In the region with low longitudinal unit conductance, its values ranges from 0.05 to 0.22 Ohm.m<sup>2</sup> and in the region with higher unit conductance its values ranges from 0.14 to 0.26 Ohm.m<sup>2</sup>. The contour pattern and boundaries are unique clear and display overlapping features.

Longitudinal unit conductance is related to clay content. It increases towards the North, which indicates increase in porosity of the layer but

decreases its permeability. Towards the west, there is decrease in the high absorption and retention capacity

#### 4.8. Bedrock relief map

Figure 24 demonstrates contour pattern of the bedrock map of the fresh bedrock elevation in all the VES stations. These elevations were obtained by removing the overburden thickness of the bedrock topography and its structural disposition. The hydro geologic relevance of bedrock relief has been recognised by Olorunfemi and Okhue (1992); Olorunfemi and Olorunniwo 1985; Dan-Hassan and Olorunfemi (1999) and Omosuyi et al. (2003).

Topographic depression and ridges are identified in the bedrock relief map. Basement is high towards the west and decreases towards the east. Depression is characterised by thick overburden while ridges are noted for thin overburden cover. Basement depressions forms groundwater collecting trough, especially water displaced from crest.

##### 4.8.1. Resistivity of the bedrock

The contour map (Figure 25) of the bedrock resistivity has resistivity values of the bedrock ranging from

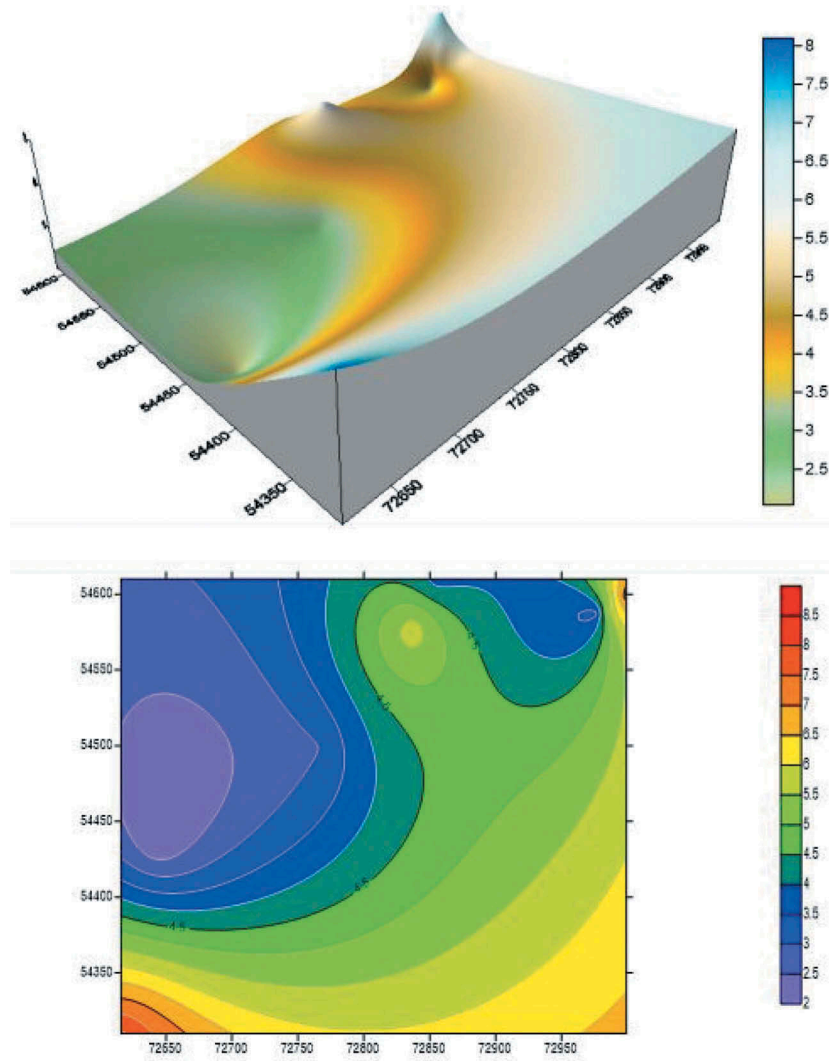


Figure 20. 3D Contour map of the weathered layer hydraulic conductivity.

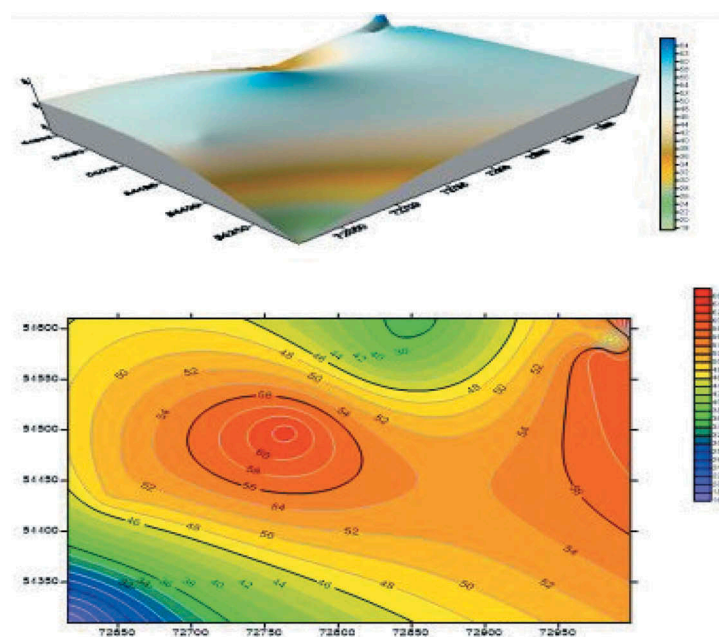


Figure 21. 3D Contour map of the weathered layer transmissivity.



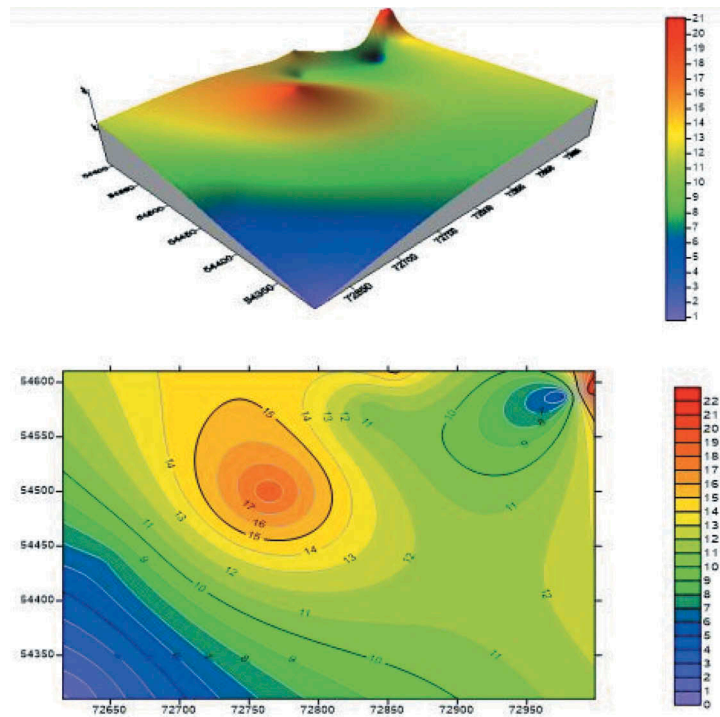


Figure 22. 3D Contour map of the weather layer overburden.

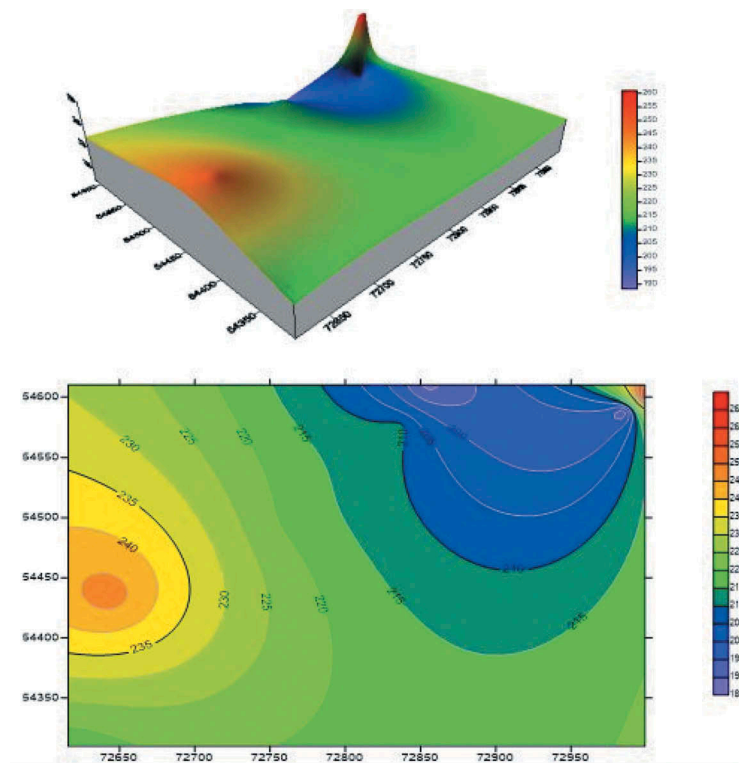


Figure 23. 3D Contour map of the weather layer longitudinal unit conductance (s).

223.4 to 1564 Ohm.m<sup>2</sup>. According to Olayinka and Olorunfemi 1992, the resistivity values that exceed 100 Ohm.m is of fresh bedrock but where the resistivity reduces to less than 1000 Ohm.m, the bedrock is fractured zone forms a major constituent of aquifer in a basement complex terrain. Researchers

authenticates that shallow buried such as metamorphic rocks gives high resistive stripe – shape contours while that shallow buried bedrocks such as low resistive stripe – shape contours (Olorunfemi and Okhue 1992; Olorunfemi and Opadokun 1986; Dan-Hassan and Olorufemi 1999 and Omosuyi et al 2003).

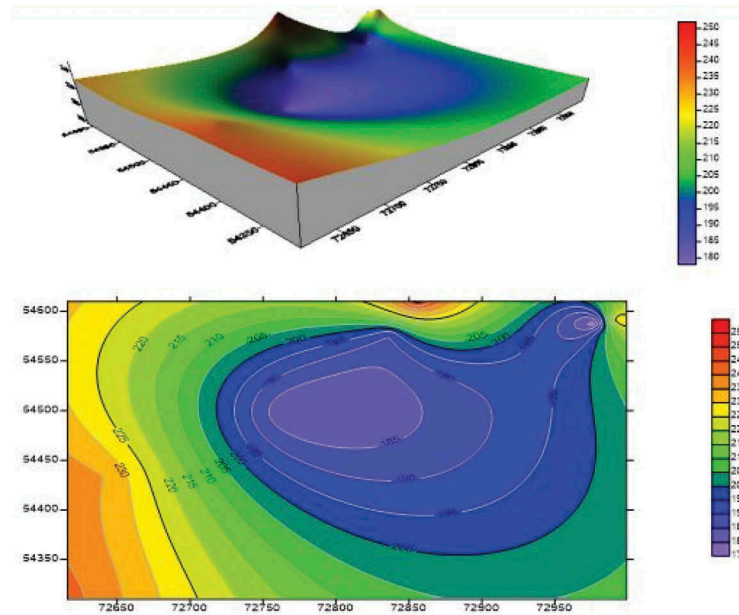


Figure 24. 3D Contour map of the weathered layer bedrock relief.

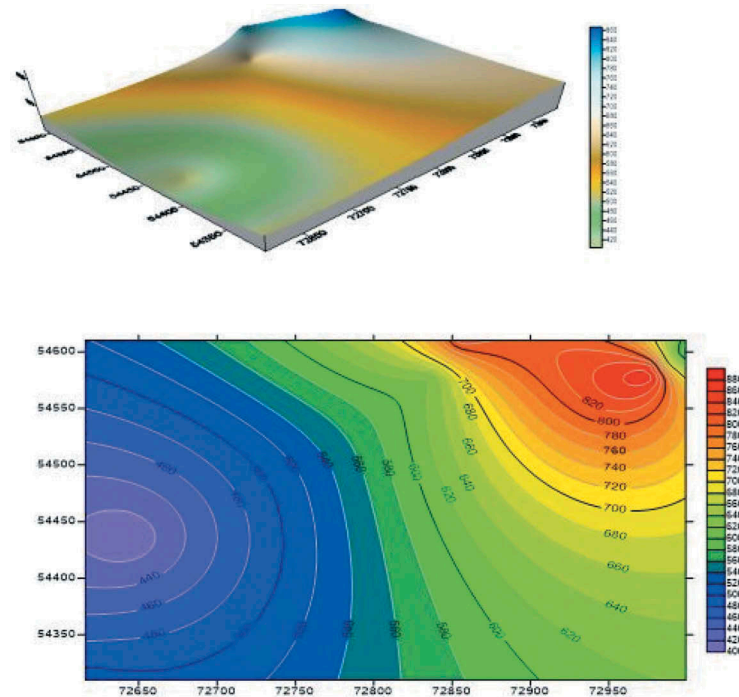


Figure 25. 3D Contour map of the weather layer resistivity of the bedrock.

Hence, it could be concluded that areas with low bedrock resistivity are areas of interest in terms of groundwater exploration in the study area.

#### 4.8.2. Total transverse resistance

A vertical stack of thickness from top to bottom and beds with resistivity and thickness as well as cross – section are proportional to the thickness and moves in the vertical direction. In porous media, total transverse resistance can be estimated from VES results using the mathematical calculation adopted by Niwas and Singhai (1981)

$$T_c = KRpl = KSp/KpT \quad (1)$$

Making R the subject of the formula

$$R = T_c/Kpl \quad (2)$$

Where R = Total transverse resistance Ohm.m<sup>2</sup>

S = Total longitudinal conductance Ohm.m<sup>2</sup>

Tc = Calculated transmissivity (m<sup>2</sup>/day)

The contour map (Figure 26) illustrates transverse resistance values ranging from (230 to 263 m<sup>2</sup>/day). The total transverse resistance has defined the weathered/fracture pattern of the rock in the study area and

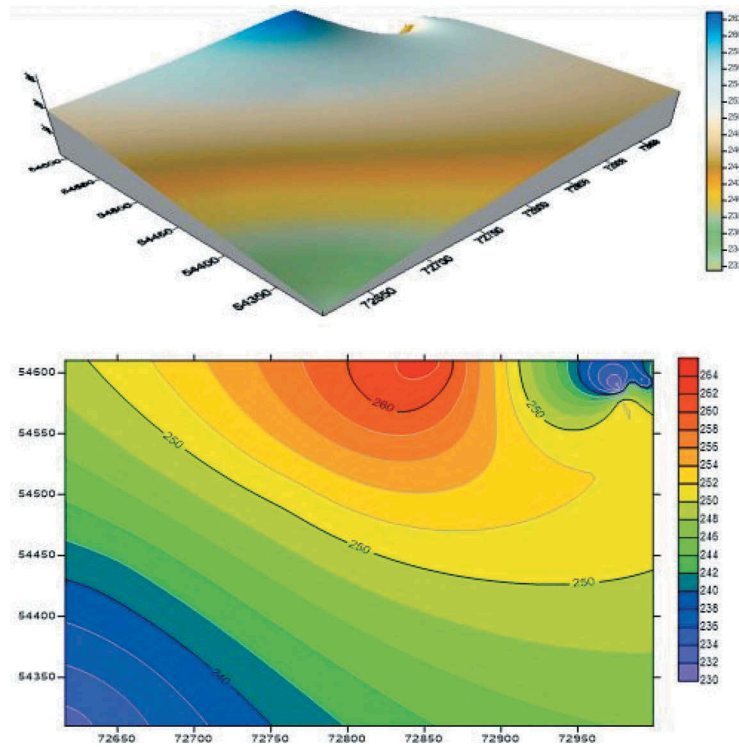


**Figure 26.** 3D Contour map of the weather layer total transverse resistance.

their thickness. Hence, defining the good aquiferous potential units in the study area.

## 5. Conclusion

This research work has extensively analysed the application of EM technique as a tool in structural mapping of the study area, the area as a result of the established trend of fractures indicate the hydro geological condition which estimates its groundwater potential and implications. The EM method has been proved to be effective in the evaluation of groundwater potential of the study area especially after the early results obtained was validated by the deployed VES technique.

It could be deduced that the VESs carried out at traverse 3 (160 m & 220 m), traverse 6 (100 m) and traverse 7 (250 m) which were on the conductive zones were all indicative of good groundwater potential while those on the non-conductive zones i.e. on traverse 7(300 m) and traverse 8 (215 m) were characterised with poor indication to groundwater potential of the zones.

The result obtained using the VES technique has established a viable significance of the conductive zone to the vast accumulation of groundwater in a typical basement complex like the study area.

This development is not limited to groundwater study alone but can also serves as a guide for follow-up work like environmental studies, engineering investigations and so on, it should also serve as a reference guide to future geophysical investigation of the area using other relevant geophysical methods.

## Acknowledgements

The authors are grateful to Adekunle Ajasin University, Akungba-Akoko, Nigeria for the release of equipment for the surveys and technical expertise of Mr. Ololade O.P during the data acquisition. The anonymous reviewers are highly appreciated for their impactful reviews that improved the quality of this manuscript.

## Disclosure Statement

No potential conflict of interest was reported by the authors.

## ORCID

C. C. Okpoli  <http://orcid.org/0000-0003-2844-3244>

## References

- Adelusi AO, Adiat KAN, Amigun JO. 2009. Integration of surface electrical prospecting methods for fracture detection in precambrian basement rocks of Iwaraja area, southwestern Nigeria. *Ozean J Appl Sci.* 2(3):2009.
- Adiat KAN, Adelusi AO, Ayuk MA. 2009. Relevance of geophysics in road failures investigation in a typical basement complex of southwestern Nigeria. Akure (NI): Department of Applied Geophysics, Federal university of technology.
- Alisiobi AR, Ako BD. 2012. Groundwater investigation using combined geophysical methods. AAPG Annual Convention and Exhibition. Long Beach: California Search and Discovery, Article 40914.
- Dan-Hassan MA, Olorunfemi MO. 1999. Hydrogeophysical investigation of basement terrain in the northcentral part of Kaduna state. *Niger J Min Geol.* 35(2):189–206.

- Erram VC, Gupta G, Pawar JB, Kumar S, Pawar NJ. 2010. Potential groundwater zones in parts of Dhule District, Maharashtra: a joint interpretation based on resistivity and magnetic data. *J India Geol Congr.* 2(1):37–45.
- Fraser DC. 1969. Contouring of VLF-EM data. *Geophysics.* 34:958–967. doi:10.1190/1.1440065.
- Kaikkonen P, Sharma SP. 1997. Delineation of near surface structures using VLF and VLF-R data an insight from the joint inversion result. *Leading Edge.* 16(11):1683–1689. doi:10.1190/1.1437559.
- Karous M, Hjelt SE. 1983. Linear filtering of VLF dip measurement. *Geophys Prospect.* 31:782–794. doi:10.1111/j.1365-2478.1983.tb01085.x.
- Kearey P, Brooks M, Hill I. 2002. An introduction to geophysical exploration. 3rd ed. Oxford: Blackwell publishing; p. 262.
- Lowrie W. 2007. Fundamentals of geophysics. 2nd ed. New York (NY): Cambridge University press; p. 384.
- McNeill JD, Labson VF. 1991. Geological mapping using VLF radio fields. In: Nabighian M, editor. *electromagnetic methods in applied geophysics.* Vol. 2. Tulsa (OK): Society of Exploration Geophysicists. p. 521–640.
- Milsom J. 2003. *Field geophysics.* 3rd ed. England: John Wiley & Sons; p. 249.
- Niwas S, Singhai DC. 1981. Estimation of aquifer transmissivity from Dar-Zarrouk parameters in the porous media. *J Hydrol.* 50:393–399. doi:10.1016/0022-1694(81)90082-2.
- Okpoli CC. 2017. Hydrogeochemistry of water resources of Oka municipality. *Geosci Res.* 2(1):46–58. doi:10.22606/gr.2017.21006.
- Okpoli CC, Odundun OA. 2016. Investigation of groundwater vulnerability due to leachate infiltration in Iwaro-Oka region, Nigeria using geochemistry and electrical resistivity tomography. *Int Basic Appl Res J.* 2(8):48–66.
- Okpoli CC, Tijani R. 2016. Electromagnetic profiling of Owena Dam, Southwestern Nigeria, using very-low-frequency radio fields. *RMZ – M&G.* 63:237–250.
- Olayinka AI, Olorunfemi MO. 1992. Determination of geoelectrical characteristics in Okene area and implications for borehole siting. *J Min Geol.* 28(2):403–412.
- Olorunfemi MO, Okhue ET. 1992. Hydrogeologic and geologic significance of geoelectric survey at Ile-Ife, Nigeria. *J Min Geol.* 28(2):221–229.
- Olorunfemi MO, Olarewaju VO, Alade O. 1991. The electrical anisotropy and groundwater field basement complex area of southwestern Nigeria. *J Afr Earth Sci.* 12:467–472. doi:10.1016/0899-5362(91)90138-O.
- Olorunfemi MO, Olorunniwo MA. 1985. Geoelectric parameters and aquifer characteristics of some parts of southwestern Nigeria. *Geol Appl Hydrogen.* XX(1):99–109.
- Olorunfemi MO, Opadokun MA. 1986. On the application of surface geophysical measurement in geological mapping – basement complex of southwestern Nigeria as a case study. *J Afr Earth Sci.* 6(3):287–291. doi:10.1016/0899-5362(87)90071-6.
- Omosuyi GO, Enikanselu PA. 1991. Direct current resistivity sounding for groundwater potential in basement complex of North-Central Nigeria. *J Sci Eng Technol.* 2(1):331–334.
- Omosuyi GO, Ojo JS, Enikanselu PA. 2003. Geophysical investigation for groundwater around Obanla-Obakekere in Akure area within the basement complex of southwestern Nigeria. *J Min Geol.* 39(2):109–116.
- Orellana E, Mooney HM. 1972. Two and three-layer master curves and auxiliary point diagrams for vertical electrical soundings using Wenner arrangement. Madrid (Spain): Interciencia 43 sheets.
- Rahaman MA. 1988. Recent advances in the study of the basement Complex of Nigeria. *Geological Survey of Nigeria.* 11–41.
- Rahaman MA, Ocan O. 1978. On the relationships in the precambrian magmatic gneisses of Nigeria. *Precambrian Geology of Nigeria Volume 1.* *J Min Geol.* 15:23–32.
- Reynolds JM. 1997. *An introduction to applied and environmental geophysics.* Chichester: Wiley. p. 806.